CRP Subunit Association and Hinge Conformation Changes in Response to cAMP Binding: Analysis of C-Helix Cysteine-Substituted CRP†

Steven R. Tomlinson,‡ Yusuf Tutar,‡,§ and James G. Harman*,‡,||

Department of Chemistry and Biochemistry, Texas Tech University, Lubbock, Texas 79409, Department of Chemistry, Cumhuriyet University, Sivas, Turkey 58140, and Chemistry Department, South Plains College, Levelland, Texas 79336

Received May 31, 2006; Revised Manuscript Received September 11, 2006

ABSTRACT: We investigated the characteristics of 13 CRP variants having cysteine substituted at positions 113, 115, 116, 117, 118, 120, 122, 124, 126, 127, 129, 130, or 131, positions that span the length of the CRP C α-helix. Under reducing conditions, the WT and all Cys-substituted forms of CRP migrated as 23.5 kDa CRP monomer species on SDS−PAGE gels. In the absence of a reductant, 9 of 13 Cys-substituted forms of CRP including the L113C, S117C, M120C, L124C, V126C, T127C, E129C, K130C, and V131C CRP contained protein that migrated as 47 kDa CRP dimer species on SDS−PAGE gels. CNBr digestion of the protein preparations followed by MALDI-TOF MS analysis of the peptide fragments showed these 47 kDa species to be CRP dimers that originated from disulfide bonds formed between positional-pair C α-helix Cys residues. The ratio of monomer CRP and disulfide cross-linked CRP within a Cys-substituted CRP preparation was found to be independent of cAMP for Cys-substituted CRP preparations denatured and renatured in the presence of various cAMP concentrations. This finding suggests that there is no large-scale concerted motion (i.e., scissoring) of the CRP subunits in response to cAMP binding. In addition, we have identified three amino acid residues located along the CRP C α-helix that play a role in facilitating the conformation transition of the CRP hinge from that characteristic of apo-CRP to that characteristic of the CRP•cAMP complex.

Cyclic 3′,5′-adenosine monophosphate (cAMP)[1] plays an important role in regulating the activity of nearly 200 genes in *Escherichia coli* (*1*). The effects of cAMP are mediated through its binding to and allosteric modification of the cAMP receptor protein (CRP) (*2*). CRP is a 47238 Da dimer composed of identical 209 amino acid subunits, each of which can bind cAMP (*3*−*7*). At micromolar concentrations, cAMP binding produces conformational changes in CRP that result in a modest increase in CRP subunit stability, affect the susceptibility of CRP hinge region peptide bonds to protease, introduce CRP site-specific DNA binding, and promote CRP interaction with RNA polymerase (RNAP) (*8*−*13*).

The cyclic AMP•CRP complex structure (i.e., lg6n) has been determined from the analysis of X-ray data derived from CRP crystals grown in the presence of cAMP (*14*, *15*). Each CRP subunit folds into two domains connected by a short, random-coil hinge. The large amino-proximal domain contains three α-helices (designated A, B, and C) and extensive *β*-sheet structure which folds to form a high-affinity cAMP binding pocket. The smaller carboxyl-proximal domain is composed principally of three α-helices (designated D, E, and F), two of which, the E and F helices, form the DNA binding surface of CRP. In addition, the carboxyl-proximal domain contains a second, low-affinity, cAMP binding site.

Recent evidence shows that the identical high-affinity sites fill in the micromolar range of cAMP, exhibit positive cooperativity in cAMP binding, and have binding constant values of approximately 1×10^5 and 2×10^5 M^{-1}, respectively (*16*, *17*). The low-affinity sites fill in the millimolar range of cAMP (*16*, *17*). The structural changes induced in CRP upon binding cAMP include changes in the cyclic nucleotide binding domain, the DNA binding domain, and the interdomain hinge region and in regions involved in CRP intersubunit interaction (*18*−*20*).

Many of the subunit−subunit contacts in the CRP dimer occur between the two large domains via the two 24-residue C α-helices that extend the full length of the large N-proximal domains. The helices are packed with an interhelical angle of approximately 20° and have a slight negative superhelical twist allowing them contact along their entire length (*5*, *14*, *15*). It has been proposed that the interaction of cAMP with amino acids in the cyclic nucleotide binding pocket initiates cAMP-mediated changes in CRP conformation that are likely to include reorientation of CRP subunits (*5*, *14*, *21*).

Interactions involving both the methyl and the hydroxyl group of T127 appear to play important roles in establishing

†This work was funded by the Robert A. Welch Foundation (Grant D-1248) and through seed grants from the Texas Tech University Graduate School and the Texas Tech University Institute for Biotechnology.

* Corresponding author. Phone: 806-894-9611 ext 2327. Fax: 806-894-5274. E-mail: jharman@southplainscollege.edu.

‡ Texas Tech University.

§ Cumhuriyet University.

|| South Plains College.

[1] Abbreviations: cyclic AMP or cAMP, cyclic 3′,5′-adenosine monophosphate; CRP, cAMP receptor protein; *lac*P, lactose operon promoter; RNAP, RNA polymerase; ANS, 8-anilino-1-naphthalenesulfonic acid; MALDI-TOF MS, matrix-assisted laser desorption/ionization time of flight mass spectrometry.

10.1021/bi0610855 CCC: $33.50
Published on Web 10/20/2006

the CRP hinge conformation in the absence of effector and in stabilizing the apo-CRP structure (*22*). Mutations that eliminate the T127 methyl, hydroxyl, or both produced CRP mutants that showed either no or limited transcription activation activity in the presence of cAMP (*22*). One mutant, the T127C CRP, was shown to establish an intermolecular disulfide cross-link between CRP subunits and was fully functional in the presence of cAMP. If a subunit scissoring motion is involved in CRP activation, the fact that T127C CRP was fully functional and cross-linked suggests that position 127 provides a pivot point for this subunit realignment. It is this predicted motion in CRP that is the focus of the work reported here.

We have monitored reorientation of the C α-helices in CRP through the ability of positional-pair cysteine residues to form disulfide bonds in apo-CRP, in the CRP•$(cAMP)_2$ complex, and in the CRP•$(cAMP)_4$ complex. It was expected that the C helices of CRP would adopt, in the presence of millimolar concentrations of cAMP, the orientation observed in CRP•$(cAMP)_4$ crystals. In this conformation of CRP, it was predicted that cysteine residues substituted at positions 113, 114, 117, 120, 121, 123, 124, 127, 128, 130, and 131 will form intermolecular disulfide bonds. Cysteine residues at positions 115, 116, 118, 119, 122, 125, 126, and 129 were not expected to form disulfide bonds under these conditions. If scissoring of the C α-helices does result from interconversion of the three forms of CRP, then we predicted that the distribution of intermolecular disulfide bonds would be cAMP-dependent. In addition, biochemical characterization of Cys-substituted CRP has revealed a pathway for signal transfer from the cyclic nucleotide binding pocket to the CRP hinge.

MATERIALS AND METHODS

Bacterial Strains and Plasmids. *Escherichia coli* CA8445/pRK248 (*23*) was used as host strain for recombinant *crp* plasmids. Plasmid pRK248 (λcI^{ts}, tet^r) (*24*) encodes a thermolabile λcI repressor used to control the λP_L promoter. Plasmid pLEX (Invitrogen) was used for high-level WT and mutant CRP expression. Plasmid pHA7 (*3*) and its C-helix Cys-substituted CRP derivatives were used to assess the effect of amino acid substitutions on CRP efficacy in stimulating *lac*P activity in vitro.

Enzymes and Other Materials. Restriction enzymes were obtained from New England Biolabs. Shrimp alkaline phosphatase, phenylmethanesulfonyl fluoride (PMSF), and isopropyl thio-β-D-galactopyranoside (IPTG) were purchased from United States Biochemical Corp. Cyclic AMP and subtilisin BPN′ (type XXVII, 7.9 units/mg) were purchased from Sigma Chemical Co. Precast 10−20% polyacrylamide gels were purchased from Bio-Rad Laboratories. DNA isolation kits were purchased from Qiagen and from Promega. Synthetic oligonucleotides were synthesized by the Texas Tech University Biotechnology Institute Core Facility. Common salts and buffers were of reagent grade or better.

Site-Directed Mutagenesis of CRP. Double-stranded plasmid DNA was mutagenized using the Quick-Change PCR protocol (Stratagene) coupled with the mutagenic oligonucleotide pairs listed in Supporting Information, Table 1.

Assay of β-Galactosidase. CA8445/pRK248 cells harboring pHA7 or its C-helix Cys-substituted CRP derivatives were cultured as described by Belduz et al. (*25*). Samples were assayed for β-galactosidase activity according to Miller (*26*).

CRP Isolation. CRP was prepared using standard ion-exchange chromatography techniques. CRP induction, extract preparation, and purification over Bio-Rex 70 resin were carried out as described by Harman et al. (*23*).

Protein Preparation. Aliquots of WT and Cys-substituted forms of CRP contained in SPECTRA/POR RC Sterile DispoDialyzer tubes (MWCO: 15000) were dialyzed against 20 volumes of low salt buffer (LSB) that contained 5 M urea and 10 mM β-mercaptoethanol (β-ME) for 6 h. The dialysis buffer was replaced, and dialysis was continued an additional 6 h. The protein samples were divided into three aliquots and dialyzed for 6 h against 20 volumes of LSB containing 5 M urea, 10 mM β-ME, and either no cAMP (aliquot 1), 50 μM cAMP (aliquot 2), or 5 mM cAMP (aliquot 3). Protein preparation was concluded with dialysis against 20 volumes of LSB that contained the appropriate cAMP concentration and lacked β-ME for an additional 6 h. Protein samples were stored at −80 °C.

CRP Cross-Linking. CRP (5.0 μg) prepared as described was diluted 1:2 in nonreducing SDS−PAGE sample buffer. The samples were heated to 70 °C for 3 min and clarified by centrifugation at room temperature at 10000 rpm for 1 min. The proteins were separated on nonreducing 10−20% Tris-HCl gels and visualized by staining with acidic Coomassie blue R-250, and the amount of dimer and monomer in each sample was quantitated using a Molecular Dynamics 300B laser densitometer.

MALDI-TOF MS. Selected protein samples were diluted in 2 volumes of the ionizing matrix that was 10 mg/mL in sinnapinic acid, 0.3% in TFA, and 50% in acetonitrile. Aliquots of this mixture were then analyzed using a Voyager DE MALDI-TOF MS (PerSeptive, Cambridge, MA). Spectra consisted of 64 single-shot analyses that were averaged for improved signal-to-noise ratios.

Disulfide Mapping. Partial CNBr digestion reactions were performed as described by Matsudaria (*27*). Reaction mixtures contained 30 μg of CRP in 70% formic acid. Cleavage reactions were initiated by the addition of 30 μL of 5 M CNBr dissolved in acetonitrile. The reactions were incubated in the dark at 23 °C for 2 h and terminated by the addition of 1.0 mL of H_2O. Lyophilized peptides were resuspended in H_2O and dialyzed against 1000 volumes of H_2O using SPECTRA/POR Molecular porous membrane tubing (MWCO: 1000). The peptides were again lyophilized and dissolved in 20.0 μL of H_2O prior to MALDI-TOF MS analysis.

Protease Probe of CRP Structure. Protease digestion reactions containing 20 μg of CRP and, where indicated, cAMP were run at 23 °C in a volume of 40 μL in NP buffer that was 100 mM in NaCl as described previously (*25*). Peptides were resolved on 10−20% gradient polyacrylamide−SDS gels, visualized by staining with acidic Coomassie blue R-250, and quantitated using a Molecular Dynamics 300B laser densitometer.

Cyclic AMP Binding Assay. Fluorescence titration experiments were conducted at room temperature on protein samples that had been dialyzed against 50 mM Tris-HCl (pH 7.8), 0.1 M KCl, and 1.0 mM EDTA. All fluorescence measurements were performed on a SLM 4800C spectro-

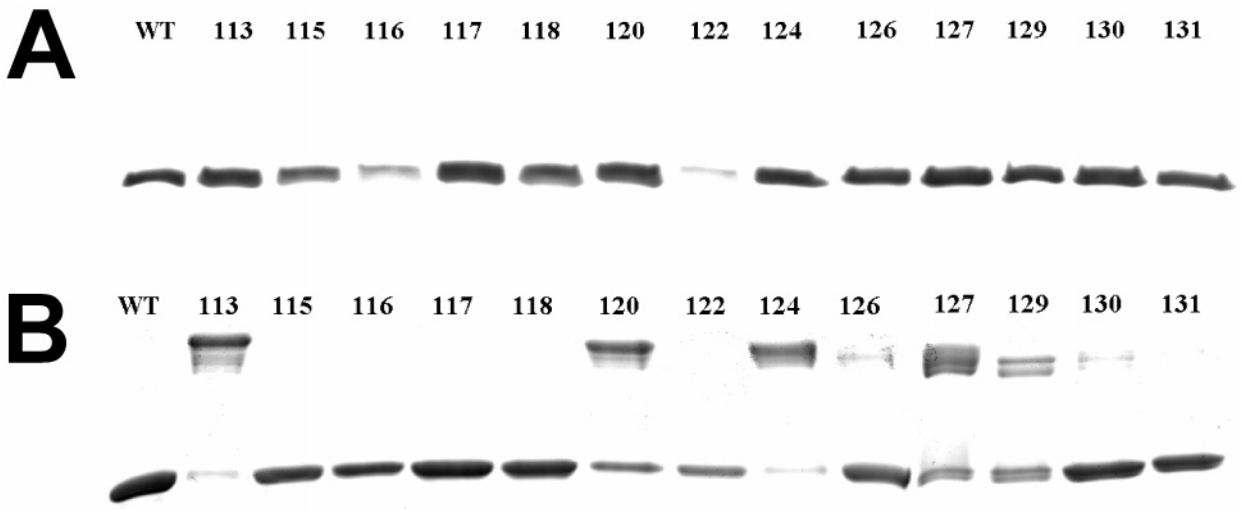

FIGURE 1: SDS−PAGE of WT CRP and Cys-substituted forms of CRP prepared as described in Materials and Methods. The position of Cys substitution is shown above each lane. Panel A: SDS−PAGE run in the presence of reducing agent. Panel B: SDS−PAGE run in the absence of reducing agent.

fluorometer. The binding of cAMP to ANS-CRP was studied by the sequential addition of 2−15 μL volumes of concentrated cAMP to a 1.0 mL solution of CRP (5.0 μM) that contained 15 μM ANS. The excitation and emission wavelengths were set at 350 and 480 nm, respectively. The data were corrected for the fluorescence of free ANS in cAMP titration experiments where CRP was omitted from the buffer solution. ANS cAMP titration data, where two components were evident in the cAMP binding isotherm, were analyzed according to the two-component model of Heyduk and Lee (*7*), which provides an accurate measure of the association constant value K_{app}^{cAMP1} (*17*).

RESULTS

Disulfide bonds can form between Cys residues if the α-carbon atoms are within 4−9 Å and the polypeptide backbones are oriented to allow nearly direct approach of the Cys side chains (*28*−*30*). We have monitored the formation of positional-pair disulfide bonds between subunits in Cys-substituted CRP to assess the relative orientations of the C α-helices for CRP exposed to different concentrations of cAMP. We previously found that the T127C CRP disulfide bond, located at the CRP subunit interface, was accessible to solvent only under denaturing conditions (*31*). With this in mind, along with the fact that CRP is reversibly denatured in the presence of 5 M urea (*9*), we chose to denature the WT CRP and Cys-substituted forms of CRP under reducing conditions, introduce cAMP, and, through buffer exchange, renature the proteins in the presence of cAMP under conditions where both the denaturant and the reductant were dialyzed out of solution. In developing this strategy to probe concerted CRP subunit motion in response to cAMP binding, we made the following assumptions: first, that apo-CRP and the CRP·$(cAMP)_2$ complex maintain a C-helix structure similar to that observed in the CRP·$(cAMP)_4$ complex (*14*, *15*); second, that cAMP-mediated change in CRP conformation includes reorientation of the C-helices; third, that a concerted reorientation of the C-helices in response to cAMP is sufficiently large to affect disulfide bond formation between positional-pair Cys residues.

Aliquots of WT and Cys-substituted forms of CRP denatured in buffer solution that contained 5 M urea and β-mercaptoethanol were renatured either in the absence of cAMP, in the presence of 50 μM cAMP, or in the presence of 5 mM cAMP. Samples of the WT and Cys-substituted CRP prepared for SDS−PAGE under *reducing* conditions were shown to contain a single protein species that migrated as a 23.5 kDa CRP monomer band (Figure 1, panel A). Protein samples prepared for SDS−PAGE under *nonreducing* conditions produced varied results (Figure 1, panel B). Renatured in the absence or in the presence of cAMP, WT CRP preparations did not form intermolecular disulfide bonds as evidenced by the absence of 47 kDa bands in nonreducing SDS−PAGE gels (Figure 1, panel B, lane 1). In contrast, several of the Cys-substituted CRP preparations contained a 47 kDa protein species on SDS−PAGE gels run under nonreducing conditions (Figure 1, panel B, lanes 2−14). Densitometry traces of individual lanes were used to quantify the amount of disulfide cross-linked dimer present in each CRP population. The results of this analysis show that a 47 kDa species made up 85% of the L113C CRP preparation, 4% of the S117C CRP preparation, 46% of the M120C CRP preparation, 73% of the L124C CRP preparation, 17% of the V126C CRP preparation, 76% of the T127C CRP preparation, 54% of the E129C CRP preparation, 17% of the K130C CRP preparation, and 13% of the V131C CRP preparation. S117C CRP, a Cys-substituted CRP that we had predicted would form intermolecular disulfide bonds at millimolar concentrations of cAMP, did not form cross-linked CRP dimers at 5 mM cAMP and only showed 4% dimer formation in the absence of cAMP and in the presence of 50 μM cAMP. V126C and E129C CRP, two Cys-substituted forms of CRP that we had predicted would not form intermolecular disulfide bonds at millimolar concentrations of cAMP, contained measurable amounts of cross-linked CRP dimer at all three concentrations of cAMP.

The data obtained for CRP renatured in the absence of cAMP and in the presence of 50 μM cAMP or 5 mM cAMP are summarized in Figure 2. We observed no significant difference in the distribution of disulfide cross-linked CRP subunits for any given CRP preparation when assayed in the absence of cAMP or in the presence of either micromolar or millimolar concentrations of cAMP.

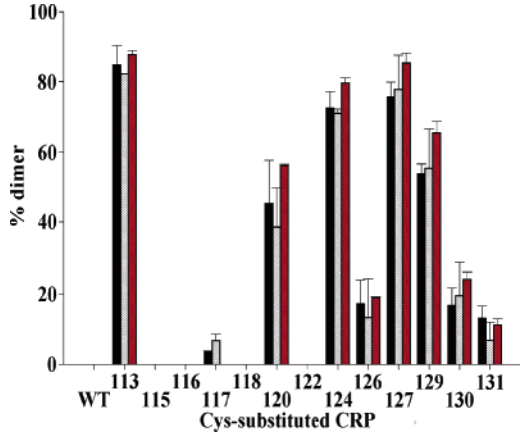

FIGURE 2: Percent dimer formation of WT and Cys-substituted forms of CRP renatured in the presence of the indicated concentration of cAMP. Renaturation was done in the absence of cAMP (black bars), in the presence of 50 μM cAMP (stippled bars), and in the presence of 5 mM cAMP (red bars).

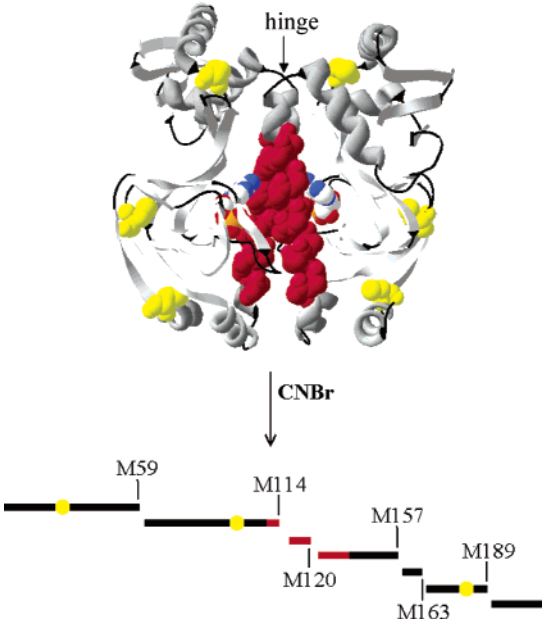

FIGURE 3: CRP ribbon structure generated from 1gn6 coordinates. The locations of naturally occurring Cys residues C18, C92, and C178 in WT CRP are identified by space-filled representations of the Cys side chains (yellow). The C α-helix, including positions 113 through 131, is shown in a space-filled representation of residue side chains (red). Cyclic AMP is presented in CPK colors. Complete CNBr cleavage of WT CRP generates seven fragments shown in a linear primary sequence representation. Met residue locations are indicated.

The WT CRP monomer contains Cys residues at positions 18, 92, and 178. Subjected to CNBr-mediated cleavage, WT CRP yields seven peptide fragments, five of which were unequivocally identified by MALDI-TOF MS under the conditions used in this study (Figure 3). The results of the SDS−PAGE analysis of WT CRP showed that during renaturation CRP monomers do not form disulfide cross-linked CRP monomers whereas several C-helix Cys-substituted forms of CRP do produce, in a position-dependent manner, protein populations that contain disulfide cross-linked dimers. Disulfide mapping experiments were conducted to determine the location of the cysteine residues participating in the intermolecular disulfide cross-links to confirm the identity of these disulfide cross-linked species

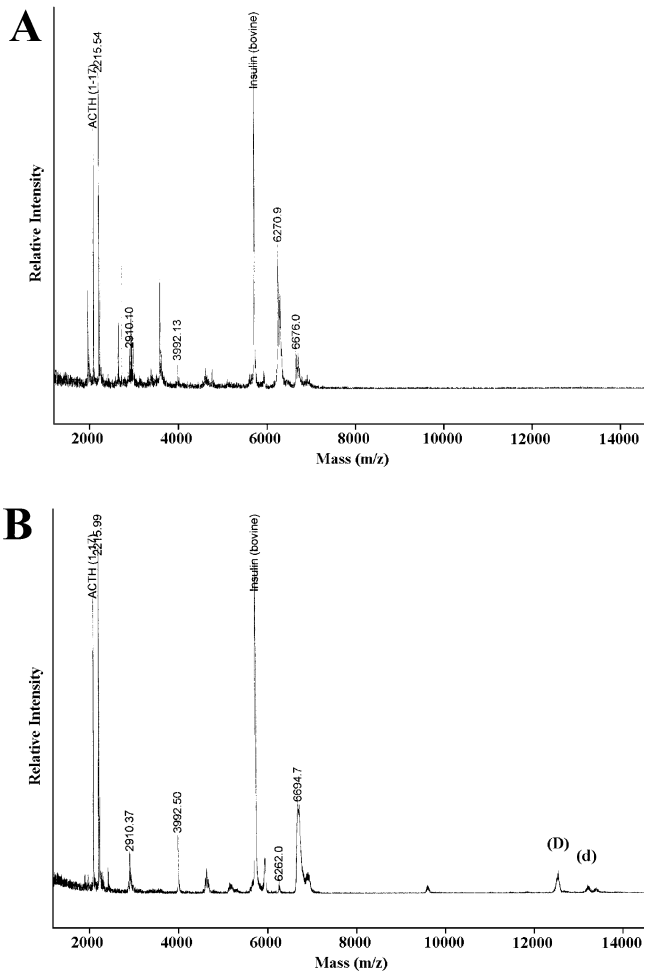

FIGURE 4: MALDI-TOF spectrum of CNBr-generated CRP peptides. The spectra were calibrated using ACTH (1−17) and insulin as internal mass standards. The *m*/*z* numbers 2215.5, 2910.1, 3992.1, 6270.9, and 6676.1 correspond to CRP peptides L190-R209, Q164-M189, A121-M157, I60-M114, and V1-M59, respectively. Panel A: CNBr-digested WT CRP. Panel B: CNBr-digested L113C CRP. The *m*/*z* peak at 12521.5 is a dimer of the I60-M114 peak and is diagnostic of position Cys 113 disulfide cross-linked peptides. There is a minor diagnostic peak at *m*/*z* 13211.2 that corresponds to disulfide cross-linked I60-M114 and I60-M120 peptides (calculated *m*/*z* of 13208.4).

as positional-pair disulfides. Partial digestion of CRP by CNBr treatment was followed by MALDI-TOF MS analysis of the peptide fragments. The molecular masses of the CRP peptides were then compared with the masses of peptides predicted from the analysis of the CRP primary structure. Covalent cross-linking of peptides produced unique and predictable molecular mass species allowing for the identification of those regions in CRP that contain the participant cross-linked amino acid residues. The results of the disulfide mapping experiments are summarized below.

(1) WT CRP preparations contained CNBr fragments having *m*/*z* peaks at 2214.7, 2909.3, 3991.2, 6269.5, and 6676.1. These peaks correspond to CRP peptides L190 through R209, Q164 through M189, A121 through M157, I60 through M114, and V1 through M59, respectively. Neither the predicted 608.7 Da peptide, composed of T158 through M163, nor the 656.8 Da peptide composed of R115 through M120, was identified in these studies (Figure 4, panel A).

(2) L113C CRP preparations contained CNBr fragments having *m*/*z* peaks at 2214.6, 2908.9, 3989.6, 6262.2, and 6681.7 and a unique *m*/*z* peak at 12509.3. The 12509.3 peak is diagnostic for the dimer I60 through M114 peptide formed as the result of positional-pair Cys113 cross linking (Figure 4, panel B).

(3) S117C CRP preparations, which showed minimal disulfide cross-linking, contained CNBr fragments having *m*/*z* peaks at 2214.5, 2910.5, 3991.1, 6268.9, and 6676.0.

(4) M120C CRP preparations contained CNBr fragments having *m*/*z* peaks at 2214.5, 2909.3, 6271.0, and 6677.1 and unique *m*/*z* peaks at 4649.8 and 9295.6. The 4649.8 peak is consistent with the substitution of Met120 by Cys creating a unique peptide of residues R115 through M157 with a predicted mass of 4651.1. The *m*/*z* 9295.6 peak results from Cys120 positional-pair disulfide bond dimerization of peptide R115 through M157.

(5) L124C, V126C, T127C, and E129C CRP preparations contained CNBr fragments having *m*/*z* peaks at 2214.6 ± 0.02%, 2909.4 ± 0.08%, 3993.0 ± 1.8%, 6270.0 ± 0.04%, and 6677.8 ± 0.07% and a unique peak at 7980.0 ± 0.9%. The *m*/*z* 7980.0 ± 0.9% peaks are the predicted mass of A121 through M157 fragment dimers and diagnostic of an intermolecular cross-link involving Cys124, Cys126, Cys127, or Cys129 positional-pair disulfide bonds.

(6) K130C CRP and V131C CRP preparations contained CNBr fragments having *m*/*z* peaks at 2214.5 ± 0.9%, 2908.4 ± 0.03%, 4042.7 ± 0.04%, 6269.7 ± 0.00%, and 6677.0 ± 0.00%. In addition, partial digestion peaks corresponding to fragment R115 through M157 cross-linked to fragment R115 through M163 (*m*/*z* 8615 ± 0.06%), fragment R115 through M163 cross-linked to fragment R115 through M163 (*m*/*z* = 9207.8 ± 0.02%), and fragment R115 through M157 cross-linked to fragment A121 through M189 (*m*/*z* = 11513.2 ± 0.01%). All three peaks are diagnostic for an intermolecular cross-link involving Cys130 positional-pair disulfide bonds as well as Cys131 positional-pair disulfide bonds.

It is clear from the results of MALDI-TOF MS analysis of the CNBr-generated peptides from the cross-linked CRP species that cross-linking resulted from positional-pair disulfide bond formation.

The effects of C α-helix Cys substitutions on CRP structure and function were evaluated (a) through in vivo assay of β-galactosidase induction to quantitate CRP-mediated lactose operon promoter (*lac*P) activation, (b) through measurement of CRP·cAMP binding parameters, and (c) through a protease probe to monitor CRP hinge response to cAMP binding.

Cultures of CA8445 that contained either WT or a Cys-substituted CRP grown in the absence of cAMP synthesized basal levels of β-galactosidase (Figure 5, panel A). Cells that contained a Cys-substituted CRP synthesized β-galactosidase at levels that were between 60% to 113% of those observed in cells that contained the WT CRP when grown in the presence of 5 mM cAMP, with the exception of the L124C, E129C, and K130C CRP (Figure 5, panel B). Cells that contained the L124C, E129C, or K130C CRP synthesized levels of β-galactosidase that were 31%, 41%, and 5% of the level measured in cultures of WT CRP, respectively. The effects of cyclic 3′,5′-guanosine monophosphate (cGMP) addition to the culture medium was measured to assess the effect of amino acid substitutions on CRP effector specificity.

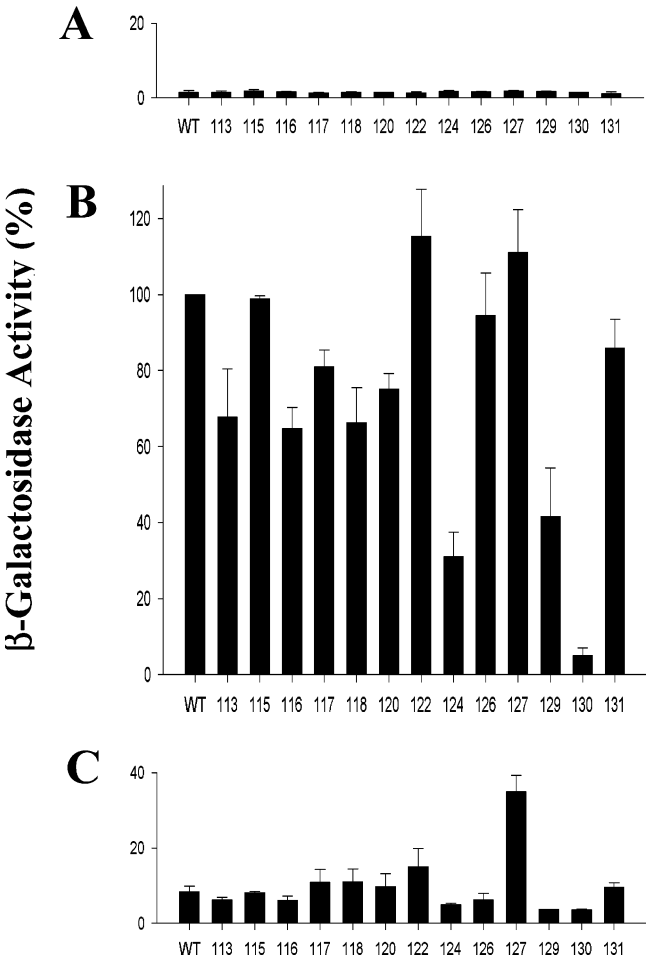

FIGURE 5: β-Galactosidase activity in cells that contained the WT or Cys-substituted forms of CRP. The amount of β-galactosidase measured in each culture is shown as a percent of the amount of β-galactosidase measured in cells that contained WT CRP and grown in the presence of 5.0 mM cAMP. Panel A: β-Galactosidase activity measured in the absence of cAMP. Panel B: β-Galactosidase activity measured in the presence of 5.0 mM cAMP. Panel C: β-Galactosidase activity measured in the presence of 5.0 mM cGMP.

Cells that contained either the WT CRP or a Cys-substituted CRP, with the exception of T127C CRP, cultured in the presence of cGMP synthesized near-basal levels of β-galactosidase activity (Figure 5, panel C). T127C CRP has previously been shown to have relaxed effector specificity, being activated by cGMP as well as cAMP (*22*).

The apparent association constants for cAMP binding to WT CRP exhibit values that range from 3.0×10^4 to 30×10^4 M^{-1} for K_{app}^{cAMP1} (*6*, *7*, *16*, *17*, *31*). We have utilized ANS·CRP fluorescence intensity changes as a function of cAMP concentration to measure cAMP binding and fitted the data to the two-site model to determine the effects of C-helix Cys substitutions on CRP affinity for cAMP (Figure 6). K_{app}^{cAMP1} values for WT CRP and the S117C, A118C, M120C, R122C, L124C, Q129C, and K130C forms of CRP were calculated to be 3.1×10^5, 1.7×10^5, 0.9×10^5, 2.3×10^5, 1.3×10^5, 0.2×10^5, 0.7×10^5, and 0.7×10^5 M^{-1}, respectively (Figure 6). These values vary from that measured for the WT CRP by factors of 1.3−15.5 with the largest variation observed for the L124C CRP.

Protease digestion reactions have been utilized to probe structural changes that occur in CRP upon binding of cAMP

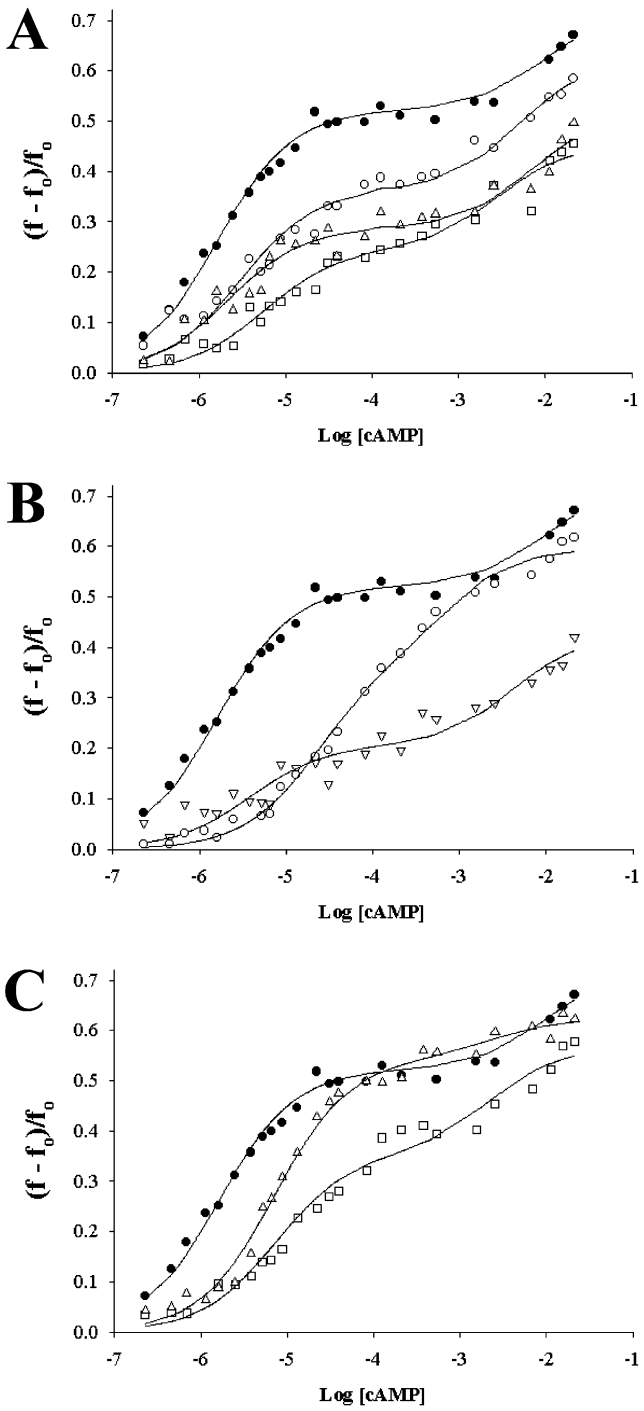

FIGURE 6: Binding of cAMP to WT and Cys-substituted forms of CRP. Fluorescence intensity of ANS·CRP complexes was measured as a function of cAMP concentration. Panel A: WT CRP (closed circles), S117C CRP (open circles), A118C CRP (open boxes), and M120C CRP (open triangles). Panel B: WT CRP (closed circles), R122C CRP (open inverted triangles), and L124C CRP (open circles). Panel C: WT CRP (closed circles), Q129C CRP (open boxes), and K130C CRP (open triangles). The data were fit to the two-component model of Heyduk and Lee (*7*). Each data point is the average of three independent experiments.

(*32*). A minimum of three different conformational states of WT CRP have been shown exist on the basis of varying sensitivity to proteases (*10*). Apo-CRP is protease resistant (Figure 7, lane 2); the CRP·$(cAMP)_2$ complex that predominates at micromolar concentrations of cAMP is protease sensitive and in the presence of protease generates a protease-resistant α-core CRP fragment (Figure 7, lane 3).

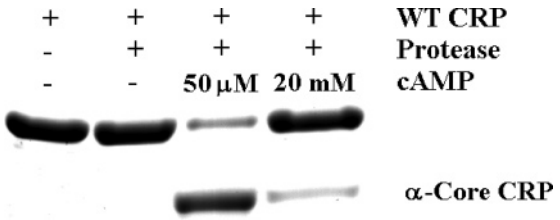

FIGURE 7: WT CRP response to protease. WT CRP was incubated with subtilisin in the absence of cAMP (lane 2), in the presence of 50 μM cAMP (lane 3), and in the presence of 20 mM cAMP (lane 4). Lane 1 is WT CRP in the absence of subtilisin.

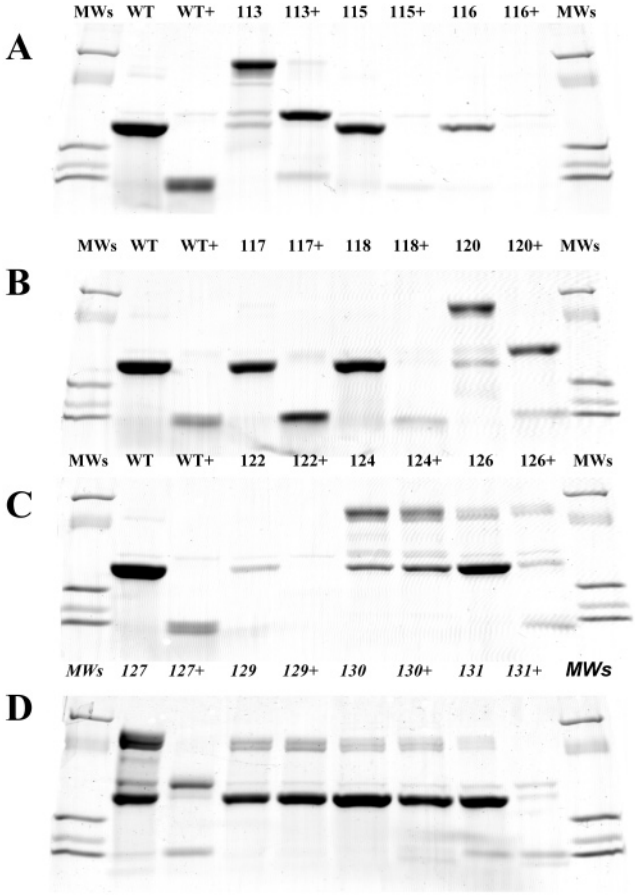

FIGURE 8: Cys-substituted CRP response to protease. WT and Cys-substituted forms of CRP were with subtilisin in the presence or absence of cAMP. Allele designations followed by a plus sign (+) indicate reactions that contained 50 μM cAMP. Lanes are labeled by the position of Cys substitution. MWs labeled lanes contain a molecular mass standard mixture of proteins that were 66, 45, 21, 18.4, and 14.3 kDa.

The CRP·$(cAMP)_4$ complex predominates at millimolar concentrations of cAMP and is less sensitive to protease digestion than is the CRP·$(cAMP)_2$ complex (Figure 7, lane 4). The α-core fragment composed of residues V2 through 116 to 130 generated by the digestion of WT CRP with protease in the presence of micromolar concentrations of cAMP remains resistant to further proteolysis as long as cAMP remains bound (*10*). Protease digestion reactions were used to monitor conformational changes in the CRP structure as a result of cAMP binding.

Each CRP population displayed a unique monomer−dimer distribution on SDS−PAGE gels (Figure 8). Ignoring the differences in CRP masses due to disulfide cross-linking of CRP or CRP core fragment subunits, each CRP sample fell

into one of four general classes of response to the protease subtilisin. The first class, represented by the WT CRP, was resistant to protease in the absence of cAMP and digested to a stable α-core fragment in the presence of 50 μM cAMP. The Cys-substituted CRP that fit into this response class included the L113C CRP, L117C CRP, M120C CRP, V126C CRP, and T127C CRP (Figure 8). The second class of CRP response to protease was observed in the R115C CRP, A118C CRP, and V131C CRP (Figure 8). These proteins were resistant to protease in the absence of cAMP and sensitive to protease in the presence of 50 μM cAMP but generated an α-core fragment that was degraded by protease in the presence of cAMP. The third class of protease response was represented by the L116C CRP and R122C CRP (Figure 8). These proteins were sensitive to protease both in the absence and in the presence of cAMP. The fourth class of CRP response to protease was characterized by resistance to protease in the absence or in the presence of 50 μM cAMP. This response to protease was exhibited by the L124C CRP, E129C CRP, and K130C CRP (Figure 8).

DISCUSSION

The results of CRP cross-linking experiments reported here demonstrate that several C-helix positions, when substituted with the amino acid Cys, predictably promote the formation of positional-pair disulfide bonds to produce subunit cross-linked forms of CRP. Significant changes in the percent cross-linked CRP dimer were not observed under conditions where the apo-CRP, the CRP·$(cAMP)_2$, or the CRP·$(cAMP)_4$ conformer was expected to predominate in solution. This leads us to conclude that the CRP C α-helices do not undergo a measurable concerted motion in response to cAMP binding and in the process of CRP activation.

On the basis of analysis of the CRP·$(cAMP)_4$ crystal structure, we predicted that, in the presence of millimolar concentrations, cAMP CRP containing cysteine at positions 113, 117, 120, 124, 127, 130, and 131 could reasonably be expected to form intermolecular disulfide bonds. Conversely, we predicted that under these same conditions CRP containing cysteine at positions 115, 116, 118, 122, 126, and 129 was not expected to form intermolecular disulfide bonds. Experimental results confirmed these predictions for 10 of the 13 positions examined. For CRP containing cysteine at positions 113, 117, 120, 124, 127, 130, and 131 the percent cross-linked CRP formed varied widely from ~10% for the S131C CRP to ~90% for the T113C CRP. It is interesting that the S117C CRP populations formed only 0% (in the absence of cAMP), 3% (in the presence of 50 μM cAMP), and 5% (in the presence of 5 mM cAMP) positional-pair disulfide cross-linked species in as much as in the CRP·$(cAMP)_2$ crystal the S117 α-carbon distance is 6.03 Å with the side chains directed toward one another across the dimer axis. For CRP containing Cys at position 115, 116, 118, 122, 126, or 129 our prediction that Cys substitution would not result in the formation of intermolecular disulfide bonds held true for positions 115, 116, 118, and 122. We did, however, observe the formation of positional-pair disulfide bonds in ~20% and ~65% of the CRP population for Cys substitution of CRP positions 126 and 129, respectively. The data suggest that the C-proximal region of the C α-helix has a degree of flexibility in solution that is not reflected in the CRP·$(cAMP)_2$ crystal.

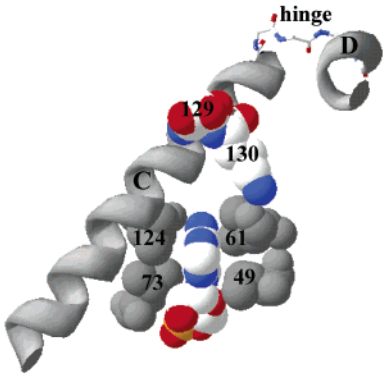

FIGURE 9: Ribbon diagram of the CRP C α-helix extending through the hinge and into the N-proximal portion of the D α-helix. Hydrophobic amino acid residues V49, L61, L79, and L124 are space-filled and colored gray. Residues Q129 and K130 and cAMP are space-filled and shown in CPK colors.

In CRP·$(cAMP)_4$ crystals, C α-helix residues 127−133 are organized as part of an α-helix whereas residues 134−139 form the flexible hinge connecting the two domains of a CRP subunit (Figure 9). There is low-resolution apo-CRP NMR data that suggest an alternative structure for the C-proximal region of the C helix beyond position 127 and extending into the CRP hinge (*20*). These NMR data indicate that residues 134−139 organize as an α-helix structure whereas C helix residues 127−133 do not. If these differences in fine structure are real, they may account for the differences between our initial predictions based on crystal structure analysis and the results of the solution-based experiments reported here.

In 1g6n, the region between positions 127 and 135 has a pattern of hydrogen-bonding interactions that include the T127 carbonyl oxygen atom bonding with the amide nitrogen atom of V131, the S128 carbonyl oxygen atom bonding with the amide nitrogen atoms of V131 and G132, the carbonyl oxygen atom of E129 bonding with the amide nitrogen atoms of G132 and N133, the carbonyl oxygen atom of K130 bonding with the amide nitrogen atoms of N133 and L134, and the carbonyl oxygen atom of V131 bonding to the amide nitrogen atom of A135. These backbone hydrogen-bonding interactions can reasonably be expected to act in concert to stabilize the CRP C α-helix/hinge boundary for the CRP·$(cAMP)_4$ complex. Experimental results from several studies show that, in the apo-form WT CRP as well as a series of CRP variants having amino acid substitutions at position 127, 128, 129, 130, or 131, the CRP hinge is protease resistant. The WT CRP·cAMP hinge is protease sensitive. However, the CRP·cAMP hinge for the variant series shows a pattern of responses to protease that is protease sensitive (position 127), protease resistant (positions 128, 129, and 130), and protease sensitive (position 131). Comparison of these CRP·cAMP hinge responses to protease and the backbone hydrogen-bonding pattern interactions for each of these positions strongly suggests that the S128, E129, and K130 carbonyl oxygen atom interactions with the G132 and N133 amide nitrogen atoms are important in the transition of the hinge response to protease from resistant to sensitive and thus in the transition of the apo-CRP hinge structure to the CRP·cAMP complex hinge structure.

In the CRP dimer, the amino acid side chain of S128 of CRP subunit A is directed into the cAMP binding pocket of

CRP subunit B. Originally thought to interact with the N^7 nitrogen atom of cAMP bound to subunit B, the finding that 7-deaza-cAMP is a potent cAMP homologue showed that this interaction was not important in cAMP-mediated CRP. However, substitution of S128 by Ala renders the CRP·cAMP complex hinge resistant to protease (*20*). The side chain of E129 is directed toward solvent; substitution of E129 by Cys renders the CRP·cAMP complex hinge resistant to protease. The side chain of K130 is buried in the large domain of the CRP subunit such that the ϵ-amino group of K130 lies within 3.11 Å of the L61 carbonyl (Figure 9); substitution of K130 by Cys renders the CRP·cAMP complex resistant to protease. Both the nature and positioning of the S128, E129, and K130 side chains are essential to the hinge conformation transition that CRP undergoes upon binding cAMP, presumably by affecting backbone hydrogen-bonding interactions important to the transition.

Studies have shown that the methyl proton resonances of CRP residues V49, L61, L73, and L124 change upon binding cAMP (*33*). We have reported that L124 plays a role in communicating cAMP binding site occupancy to the CRP hinge (*34*). We proposed in that report that, in the absence of cAMP, the nonpolar amino acid side chains that make up the cyclic nucleotide binding pocket arranged to maximize van der Waals interactions and define the cAMP binding constant K_{app}^{cAMP1}. Once bound by cAMP L124/cAMP packing interactions translate to the CRP hinge to affect cAMP-mediated allostery, a property the results presented in Figure 8 clearly demonstrate. One pathway for signal translation from the cyclic nucleotide is suggested by considering the behavior of E130C CRP.

Experimental evidence indicates that cAMP binding repositions L61 and L124 (*33*). The L61 side chain packs against one face of adenine in cAMP, and the L124 side chain packs against the opposite face of adenine in cAMP. We propose that cAMP binding repositions L61 and either establishes the L61/K130 interaction observed in CRP·$(cAMP)_4$ crystals or repositions an L61 carbonyl/K130 ϵ-amino group interaction (Figure 9). In either event this change is translated to the CRP C α-helix/hinge boundary to affect K130 carbonyl oxygen atom hydrogen bonding with the amide nitrogen atoms of N133 and L134. In the absence of the K130 side chain (e.g., K130C CRP) the CRP·cAMP complex is resistant to protease. Similarly, in the absence of the L124 side chain (e.g., L124C CRP) the CRP·cAMP complex is resistant to protease. Here, critical repositioning of L61 does not occur, and at least one important signal of cAMP binding pocket occupancy does not leave the cAMP binding pocket. As a result, the CRP hinge fails to transition from a protease-resistant to the protease-sensitive conformation characteristic of the WT CRP·cAMP complex.

SUMMARY

WT CRP-mediated control of CRP-dependent promoters requires both cAMP binding and the communication of that fact beyond the confines of the cAMP binding pocket. This report deals with two avenues by which cAMP binding pocket occupancy might be translated globally. The first mechanism involves a concerted motion, such as scissoring of the CRP subunits upon binding cAMP. Such a motion was not supported by our data; the absence of significant changes in the percentage of cross-linked CRP dimers under conditions where the apo-CRP, the CRP·$(cAMP)_2$, or the CRP·$(cAMP)_4$ conformer predominates in solution leads us to conclude that the CRP C α-helices do not undergo a concerted scissoring motion in response to cAMP binding. A second avenue supported by our data appears to involve, minimally, C α-helix residues at positions 124 and 130. These two positions, when substituted by Cys, render the CRP resistant to protease in the presence of cAMP and at least partially defective in function as a *lac*P transcription factor. The mechanism by which these positions act to complete at least one avenue of signal transfer from the cyclic nucleotide binding pocket to the CRP hinge is likely to include van der Waals packing and interaction of the K130 side chain with L61.

SUPPORTING INFORMATION AVAILABLE

One table listing mutagenic primers used to incorporate base changes in *crp*. This material is available free of charge via the Internet at http://pubs.acs.org.

REFERENCES

1. Zheng, D., Constantinidou, C., Hobman, J. L., and Minchin, S. D. (2004) Identification of the CRP regulon using *in vitro* and *in vivo* transcriptional profiling, *Nucleic Acids Res. 32*, 5874−5893.
2. Harman, J. G. (2001) Allosteric regulation of the cAMP receptor protein, *Biochim. Biophys. Acta 1547*, 1−17.
3. Aiba, H., Fujimoto, S., and Ozaki, N. (1982) Molecular cloning and nucleotide sequencing of the gene for *E. coli* cAMP receptor protein, *Nucleic Acids Res. 10*, 1345−1362.
4. Cossart, P., and Gicquel-Sanzey, B. (1982) Cloning and sequence of the *crp* gene of *Escherichia coli* K 12, *Nucleic Acids Res. 10*, 1363−1378.
5. Weber, 1.T., and Steitz, T. A. (1987) Structure of a complex of catabolite gene activator protein and cyclic AMP refined at 2.5Å resolution, *J. Mol. Biol. 198*, 311−326.
6. Takahashi, M., Blazy, B., Baudras, A., and Hillen, W. (1989) Ligand-modulated binding of a gene regulatory protein to DNA. Quantitative analysis of cyclic-AMP induced binding of CRP from *Escherichia coli* to non-specific and specific DNA targets, *J. Mol. Biol. 207*, 783−796.
7. Heyduk, T., and Lee, J.C. (1989) *Escherichia coli* cAMP receptor protein: evidence for three protein conformational states with different promoter binding affinities, *Biochemistry 28*, 6914−6924.
8. Brown, A. M., and Crothers, D. M. (1989) Modulation of the stability of a gene-regulatory protein dimer by DNA and cAMP, *Proc. Natl. Acad. Sci. U.S.A. 86*, 7387−7391.
9. Cheng, X., Gonzalez, M. L., and Lee, J. C. (1993) Energetics of intersubunit and intrasubunit interactions of *Escherichia coli* adenosine cyclic 3′,5′-phosphate receptor protein, *Biochemistry 32*, 8130−1839.
10. Eilen, E., Pampeno, C., and Krakow, J. S. (1978) Production and properties of the alpha core derived from the cyclic adenosine monophosphate receptor protein of *Escherichia coli*, *Biochemistry 17*, 2469−2473.
11. Ebright, R. H., Ebright, Y. W., and Gunasekera, A. (1989) Consensus DNA site for the *Escherichia coli* catabolite gene activator protein (CAP): CAP exhibits a 450-fold higher affinity for the consensus DNA site than for the *E. coli lac* DNA site, *Nucleic Acids Res. 17*, 10295−10305.
12. Heyduk, T., Lee, J. C., Ebright, Y. W., Blatter, E. E., Zhou, Y., and Ebright, R. H. (1993) CAP interacts with RNA polymerase in solution in the absence of promoter DNA, *Nature 364*, 548−549.
13. Busby, S., and Ebright, R. H. (1999) Transcription activation by catabolite activator protein (CAP), *J. Mol. Biol. 293*, 199−213.
14. Passner, J. M., and Steitz, T. A. (1997) The structure of a CAP-DNA complex having two cAMP molecules bound to each monomer, *Proc. Natl. Acad. Sci. U.S.A. 94*, 2843−2847.
15. Passner, J. M., Schultz, S. C., and Steitz, T. A. (2000) Modeling the cAMP-induced allosteric transition using the crystal structure of CAP-cAMP at 2.1Å resolution, *J. Mol. Biol. 304*, 847−859.

16. Scott, S.-P., and Jarjous, S. (2005) Proposed structural mechanism of *Escherichia coli* cAMP receptor protein cAMP-dependent proteolytic protection and selective and non-selective DNA binding, *Biochemistry 44*, 8730−8748.
17. Lin, S.-H., and Lee, J. C. (2002) Communications between the high-affinity cyclic nucleotide binding sites in *E. coli* cyclic AMP receptor protein: effect of single site mutations, *Biochemistry 41*, 11857−11867.
18. Baichoo, N., and Heyduk, T. (1997) Mapping conformational changes in a protein: application of a protein footprinting technique to cAMP-induced conformational changes in cAMP receptor protein, *Biochemistry 36*, 10830−10836.
19. Baichoo, N., and Heyduk, T. (1999) Mapping cyclic nucleotide-induced conformational changes in cyclicAMP receptor protein by a protein footprinting technique using different chemical proteases, *Protein Sci. 8*, 518−528.
20. Won, H.-S., Yamazaki, T., Lee, T.-W., Yoon, M.-K., Park, S.-H., Otomo, T., Kyogoku, Y., and Lee, B.-J. (2000) Structural understanding of the allosteric conformational change of cyclic AMP receptor protein by cyclic AMP binding, *Biochemistry 39*, 13953−13962.
21. Garges, S., and Adhya, S. (1985) Sites of allosteric shift in the structure of the cyclic AMP receptor protein, *Cell 41*, 745−751.
22. Lee, E. J., Glasgow, J., Leu, S.-F., Beldluz, A. O., and Harman, J. G. (1994) Mutagenesis of the cyclic AMP receptor protein of *Escherichia coli*: targeting positions 83, 127 and 128 of the cyclic nucleotide binding pocket, *Nucleic Acids Res. 22*, 2894−2901.
23. Harman, J. G., Peterkofsky, A., and McKenney, K. (1986) Structure-function analysis of three cAMP-independent forms of the cAMP receptor protein, *J. Biol. Chem. 261*, 16332−16339.
24. Bernard, H.-D., and Helinski, D. R. (1979) Use of the lambda phage promoter P_L to promote gene expression in hybrid plasmid cloning vehicles, *Methods Enzymol. 68*, 482−493.
25. Belduz, A. O., Lee, E. J., and Harman, J. G. (1993) Mutagenesis of the cyclic AMP receptor protein of *Escherichia coli*: targeting positions 72 and 82 of the cyclic nucleotide binding pocket, *Nucleic Acids Res. 21*, 1827−1835.
26. Miller, J. H. (1972) *Experiments in Molecular Genetics*, Cold Spring Harbor Laboratory Press, Cold Spring Harbor, NY.
27. Matsudaira, P. (1993) *A Practical Guide to Protein and Peptide Purification for Microsequencing*, 2nd ed., Academic Press, New York.
28. Thornton, J. M. (1981) Disulphide bridges in globular proteins, *J. Mol. Biol. 151*, 261−287.
29. Richardson, J. S. (1981) The anatomy and taxonomy of protein structure, *Adv. Protein Chem. 34*, 167−339.
30. Creighton, T. E. (1984) Disulfide bond formation in proteins, *Methods Enzymol. 107*, 305−329.
31. Leu, S.-F., Baker, C. H., Lee, E. J., and Harman, J. G. (1999) Position 127 amino acid substitutions affect the formation of CRP:cAMP:*lac*P complexes but not CRP:cAMP:RNA polymerase complexes at *lac*P, *Biochemistry 38*, 6222−6230.
32. Krakow, J. (1975) Cyclic adenosine monophosphate receptor: effect of cyclic AMP analogues on DNA binding and proteolytic inactivation, *Biochim. Biophys. Acta 383*, 345−350.
33. Lee, B.-J., Aiba, H., and Kyogoku, Y. (1991) Nuclear magnetic resonance study on the structure and interaction of cyclic AMP receptor protein and its mutants: a deuterium-labeling and photo-CIDNP study, *Biochemistry 30*, 9047−9054.
34. Tomlinson, S. R., Tutar, Y., and Harman, J. G. (2003) Interaction of CRP L124 with cAMP affects CRP cAMP binding constants, cAMP binding cooperativity, and CRP allostery, *Biochemistry 42*, 3759−3765.

BI0610855